International Journal of Scientific Research in Science, Engineering and Technology
Print ISSN: 2395-1990 | Online ISSN : 2394-4099 (www.ijsrset.com)
doi : https://doi.org/10.32628/IJSRSET229410

Hydroxyapatite integrated with Carboxymethyl cellulose and Agar-Agar/I-Carragenan biopolymer composites for antimicrobial investigations

Kiruthika T. S[1], Aravind Viswanath J[2], Jaishankar V[1]*

[1]PG and Research, Department of chemistry, Presidency College (Autonomous), Chennai, Tamil Nadu, India
[2]Department of Chemical Engineering, A.C. Tech, Anna University, Chennai, Tamil Nadu, India

Article Info
Volume 9, Issue 4
Page Number : 86-103

Publication Issue :
July-August-2022

Article History
Accepted : 01 July 2022
Published: 10 July 2022

ABSTRACT

Biopolymer based composites have been extensively used as a promising materials for various biomedical applications such as scaffold preparation, drug delivery, etc. Hence, researchers have focused their attention on the development of novel biomaterials to cater the demand in the field of medicine. In this investigation, we report the preparation and characterisation of Carboxymethyl cellulose (CMC)/Agar-Agar/n-HAp and Carboxymethyl cellulose (CMC)/I-carragenan/n-HAp polymeric composites. The common biopolymer CMC used in this study was isolated from the plant source hemp as cellulose and then it was functionalized to carboxymethyl cellulose (CMC). The SEM images showed that the addition of nano hydroxyapatite induces considerable morphological changes in the surface and cross section of the composites. Thermal analysis was used to ascertain the thermal stability of the prepared materials. Further the antibacterial, antifungal, wound healing and anticancer efficiency of the composite films were evaluated and compared. The prepared bionanocomposites have potential therapeutic value for various biomedical applications.

Keywords : Biopolymer, Carboxymethyl Cellulose, n-hydroxyapatite, Bionanocomposite, antimicrobial.

Copyright: © the author(s), publisher and licensee Technoscience Academy. This is an open-access article distributed under the terms of the Creative Commons Attribution Non-Commercial License, which permits unrestricted non-commercial use, distribution, and reproduction in any medium, provided the original work is properly cited

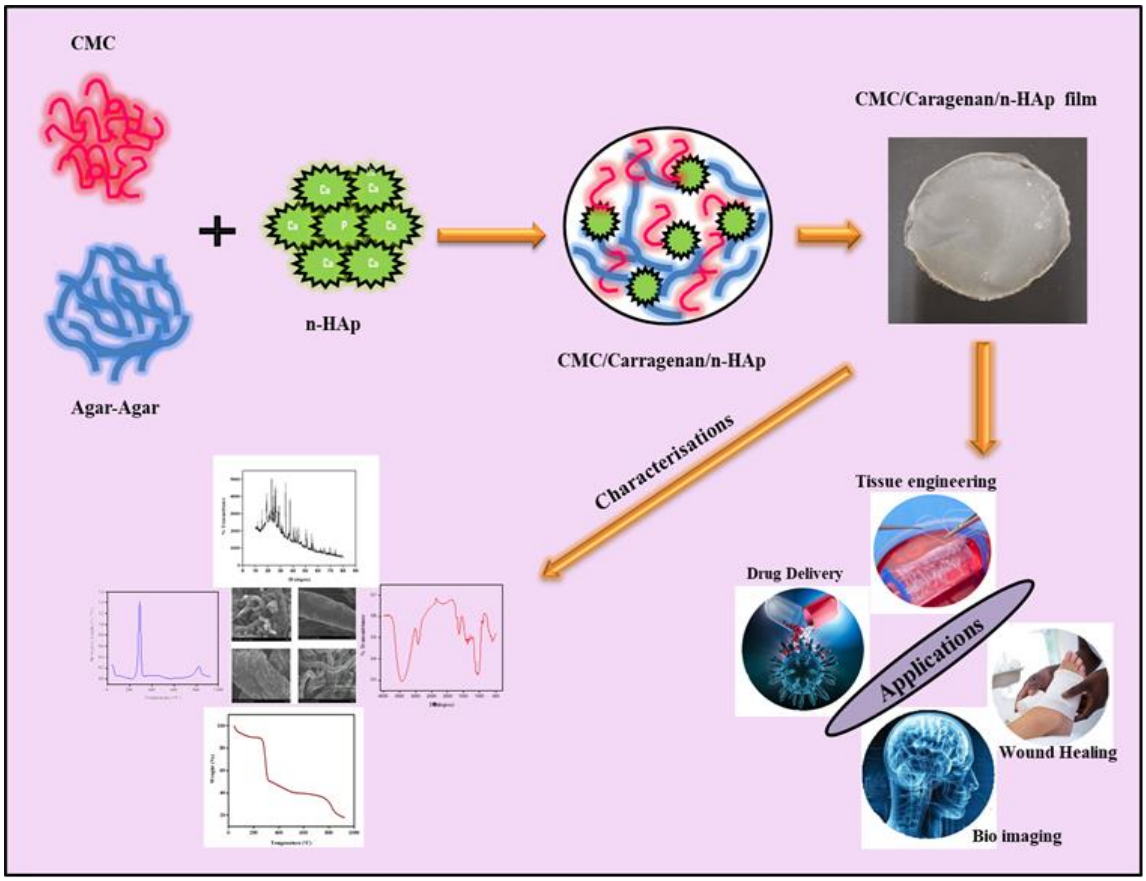

I. INTRODUCTION

The materials derived from renewable resources are increasing attention, both from the standpoint of developing innovative functional and structural macroscopic materials and from a basic scientific one [1,9,12,17]. Cellulose is a multifunctional bio-based renewable material with a variety of profitable features, including non-toxicity and biodegradability. The combination of significant value and low energy consumption makes cellulose extraction from agricultural waste is one of the best waste treatment substitutes. There are several ways for isolating and purifying cellulose, and combination of different treatments influences the shape of the fibres [2,15,22,27]. The surface area and aspect ratio of cellulose-based nanomaterials such as nano cellulose fibres, crystalline nanocellulose, cellulose composites, and so on are quite high. Wood, cotton, flax, hemp, jute, ramie, straws, sugarcane bagasse, and fruit remnants are key sources of cellulose [5,47,55]. A cellulose derived Carboxymethyl Cellulose (CMC) is a potential example of such materials that has received a lot of attention in the past two decades. CMC has been proposed for usage in a wide range of industries, including structural plastics, smart coatings, cosmetics, medicines, and solar energy gathering [7,56-59]. Strong acid hydrolysis is typically used to create these CMC particles. Extensive research has been conducted on HAp/CMC composite gels [33-37]. The use of CMC as the fibre-reinforced phase in HAp/CMC composite gels, on the other hand, has not been documented [47-53].

CMC can be employed as a thickening, binder, stabiliser, suspending agent, or flow control agent [3,26,39,43]. It is also used in the ceramic and pharmaceutical industries to cover medicinal tablets.

Because of its biocompatibility and biological characteristics, Agar-Agar (AA) and Carragenan (CA) composites are an effective artificial articular cartilage repair material. These composite films gained increasing interest in use as an articular mending material due to its high porosity structure and high concentration of free water, which is comparable to that of natural articular cartilage. With this view point, the main objective of this investigation is to isolate cellulose from hemp and its corresponding conversion into CMC. In this paper, we report the preparation, characterisation and antimicrobial studies of CMC based composites such as CMC/Agar-Agar/n-HAp and CMC/I-Carragenan/n-HAp [6,25,29,31].

II. MATERIALS AND METHODS

Raw hemp fibres scientifically named as *Cannabis sativa* was collected from local market. The obtained samples were separated from the kernels and then dried, crushed and sieved. Surface modification and bleaching were done with reagent-grade chemicals namely Sodium hydroxide, Sodium chlorite, n-Hexane, Ammonia, Sodium metabisulphite, Calcium nitrate tetrahydrate (CNT), Phosphoric acid (PA), Agar-Agar (AA), Carragenan (CA), Dimethylsulphoxide and Monochloroacetic acid (MCA).

2.1. Isolation of cellulose from hemp

Raw hemp fibers collected from local market were cleaned, dried, crushed and sieved. The desired amount of hemp fibers are soaked in 5% NaOH solution and stirred in a magnetic stirrer for 2hr [1-3]. The alkali in the fiber was removed by repeated washing with distilled water. Following the alkali treatment, the samples were bleached using acetate buffer (27 g Sodium Hydroxide and 75 mL glacial acetic acid diluted to 1 L distilled water) and aqueous Sodium Chlorite. Here the lignin content and the other non cellulosic components were removed. The slurry obtained was neutralized with acetic acid and washed with distilled water in order to maintain the neutral pH. The resultant product was dried in an air oven for 3 hours [5-7].

2.2. Preparation of Carboxymethyl cellulose (CMC)

The obtained hemp cellulose was first treated with NaOH in order to mercerize it as shown in Figure 1. Then the fibers are treated with 150 mL of ethanol solution, which is used as a solvent with magnetic stirring [4,6,8]. Then, the etherification was commenced by adding 120% of monochloroacetic acid (MCA) drop by drop with constant stirring for 30 min to maintain cellulose to liquor ratio of 1:1.2. This process was continued for another 3.5 hours at 55°C [10,11]. The resultant product obtained was supended in 200 mL of Methanol, neutralised with glacial acetic acid and and then in absolute ethanol to remove the unreacted by products. The resultant sample was dried in air oven at 60°C and used for further composite preparation and characterisation [12-16].

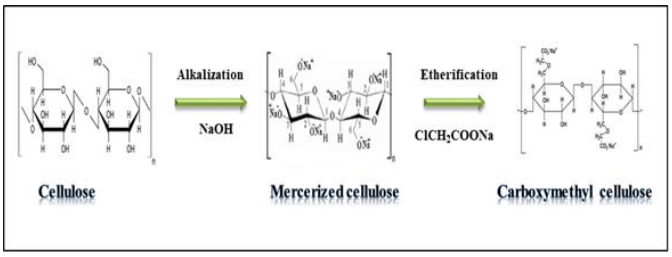

Fig 1. Synthesis of CMC from cellulose derived from hemp

2.3. Preparation of nano Hydroxyapatite (n-HAp)

Calcium nitrate tetrahydrate ($Ca(NO_3)_2{\cdot}4H_2O$) (CNT), Phosphoric acid (H_3PO_4) and Ammonia are used as starting materials for the preparation of nano Hydroxyapatite. n-HAp samples are prepared by solution precipitation method [35,36]. 1 M of Calcium nitrate tetrahydrate $Ca(NO_3)_2{\cdot}4H_2O$ was prepared and ammonia solution is added to the CNT solution in order to maintain the pH by 10. To this solution 0.25 M of Phosphoric acid was added and stirred vigorously for about 1 hr (Figure 2) gelation started. The solution is kept for aging for 24 hrs. The precipitate formed is dried in oven. The dried n-HAp powder was washed with distilled water and calcined at 500°C for 1 hr [45,46].

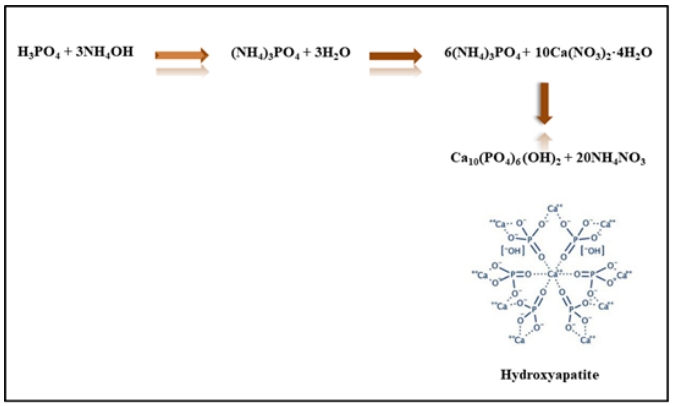

Fig 2. Synthesis of nano Hydroxyapatite

2.4. Preparation of Polymer composites

The polymeric composite CMC/AA/ n-HAp is prepared by solution casting method. The ratio of CMC:AA:n-HAp taken is 5:4:1 for the preparation. Initially, CMC from hemp and n-HAp were dissolved in hot water separately and mixed [49,50-52]. Then the mixture is stirred for about few hours. To this desired amount of Agar-Agar dissolved in double distilled were taken and added to the previous mixture. The mixture is stirred vigorously for 2 hrs and cast on a teflon petri dish and dried in an oven [53,54]. Similarly CMC/CA/n-HAp nanocomposite was also prepared [4,8,57]. The images of the composite films are presented in Figure 3.

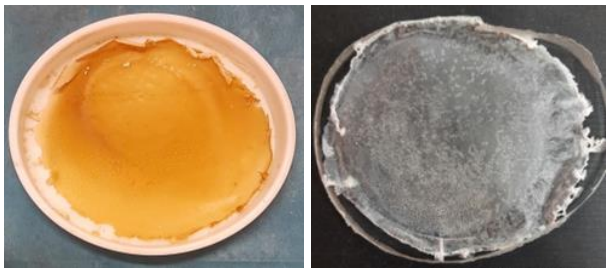

Fig 3. (a) CMC/AA/n-HAp composite film (b) CMC/CA/n-HAp composite film

III. CHARACTERISATION METHODS

3.1 IR spectral Studies

The interaction between CMC, n-HAp, Agar-Agar/Carragenan composite films was investigated using FTIR spectroscopy [1-3]. The samples were ground, mixed with KBr and pellet formed is used for the analysis. FTIR spectrophotometer was used to record the spectra in the 4000–400 cm^{-1} range.

3.2 Thermal studies

The thermogravimetric measurements were made using TGA Q500 V20.10 Build 36 thermal analyzer [4,5]. All dried samples (45 °C, 24 h) were evaluated at 30 °C/min in a nitrogen environment and at a flow rate of 30 mL/min from ambient temperature upto 930 °C.

3.3 XRD analysis

The XRD diffractograms of Cellulose (HC), CMC, n-HAp, CMC/AA/nHAp and CMC/CA/nHAp composites were recorded and analysed by Bruker D8 Advance Powder X-Ray Diffractometer [1,3,7]. The Average crystallite size of the samples was calculated using Scherrer's equation and percentage crystallinity was also calculated.

3.4 SEM analysis

The morphology of the samples was studied using Scanning Electron Microscope Quanta 400F, Inspect F, Apre0 2S instrument. The Elemental composition of materials (EDAX) was also studied by FEI QuantaTM 3D FEG equipment in order to identify the presence of elements present in the sample [2,8].

3.5 Antimicrobial studies

3.5.1 Antibacterial Activity

Stock cultures were maintained at 4°C on nutrient agar slant. Active cultures for experiments were prepared by transferring a loop full of culture from the stock cultures into the test tubes containing nutrient broth, that were incubated for 24hrs at 37°C. The assay was performed by agar disc diffusion method [22,25]. The antibacterial activity of the composites CMC/AA/nHAp and CMC/CA/nHAp was evaluated.

3.5.2 Antifungal Activity

The antifungal activity was performed for CMC/AA/nHAp and CMC/CA/nHAp composites. The stock cultures were maintained at 4°C on Sabouraud

Dextrose agar Slant. Active cultures for experiments were prepared by transferring the stock cultures into the test tubes containing Sabouraud Dextrose broth that were incubated at 48 hrs at room temperature [31-33]. The assay was performed by agar disc diffusion method.

3.5.3 Wound Healing Activity

The VERO cell line was used for Wound healing activity for composites CMC/AA/nHAp and CMC/CA/nHAp composites [11,55]. Serum free medium is used for this study.

3.5.4 Anticancer Activity

The anticancer activity was studied using MCF 7 cell line which is obtained from National Centre for Cell Sciences, Pune (NCCS). The cells were maintained in DMEM supplemented with 10% FBS, penicillin (100 U/ml), and streptomycin (100 µg/ml) in a humidified atmosphere of 50 µg/ml CO_2 at 37 °C and studied for CMC/AA/nHAp and CMC/CA/nHAp composites [41,43].

IV. RESULTS AND DISCUSSION

4.1 FT-IR Studies

Comparing the FTIR spectras of cellulose, CMC, n-HAp, CMC/AA/nHAp and CMC/CA/nHAp composite flims are shown in Figure 4. The large band observed between 3,600 and 3,200 cm^{-1} for the composite is due to the stretching of O–H from intramolecular and intermolecular hydrogen bonds in cellulose, CMC, n-HAp, CMC/AA/nHAp and CMC/CA/nHAp [2,7,18,22,36]. For CMC/AA/nHAp composites, the adsorption frequency was 2369 cm^{-1} due to the presence of PH stretching vibration. The stretching vibration of carboxylate anion caused the peak at 1750 cm^{-1}, whereas lesser intensity peaks at 1460 cm^{-1} were caused by the asymmetric deformation of CH_3. The peak at 1299 cm^{-1} shows the P=O stretching vibration. [3,44,49,51]. The peak at 1376 cm^{-1} resulted in the OH bending vibration. The peak at 1011 cm^{-1} was due to P-O-C stretching vibration, whereas the peak at 896 cm^{-1} was caused by out of plane of CH α Galactose ring of Agar in CMC/AA/nHAp. For CMC/CA/nHAp composites, The peak at 2920 cm^{-1} shows the CH stretching vibration. The peak at 1741 cm^{-1} stretching vibration of carboxylate anion. The P=O stretching vibration shows the peak at 1296 cm^{-1}. The peak at 1248 cm^{-1} shows the stretching vibration of S=O of sulphate esters. The peaks at 1011 cm^{-1} is due to P-O-C stretching vibration [4,7,11,14]. The peak at 847 cm^{-1} is for 3,6-anhydrogalactose-2-sulfate.

For CMC, the stretching frequency of the OH group causes a large absorption band at 3422 cm^{-1}, while C-H stretching vibration causes a band at 2920 cm^{-1} [5,11,17,45]. The existence of a new and strong absorption band at 1654 cm^{-1} supports the stretching vibration of carboxyl groups (COO), and carboxyl groups as salts are allocated 1423 cm^{-1} -OH bending vibration and C-O-C stretching are ascribed to the bands around 1101 cm^{-1}, respectively [7,11,22,47,53]. The peak at 1376 cm^{-1} was due to the OH bending vibration [11,44,50,56]. The 1,4-glycoside of cellulose was discovered at wavelength 896 cm^{-1} region.

For n-HAp, the peaks for PO_4^{3-} and OH^- groups in the hydroxyapatite can be identified in the peaks at 560–610 and 1000–1100 cm^{-1} must be due to PO_4^{3-} [35,36,51,52]. For the OH stretching vibration, the peak position is at 3570 cm^{-1}. The peak observed between 1654 & 1384 cm^{-1} is due to the carboxyl group salts [41,55,57]. The weakness, disappearance and shift of the characteristic absorption band might have resulted from the interactions of different OH groups in the AA and CMC molecular chains [8,22,29,34,39]. This might imply the formation of new inter- and intramolecular hydrogen bonds, as well as a change in the conformation of CMC/AA/nHAp and CMC/CA/nHAp composites.

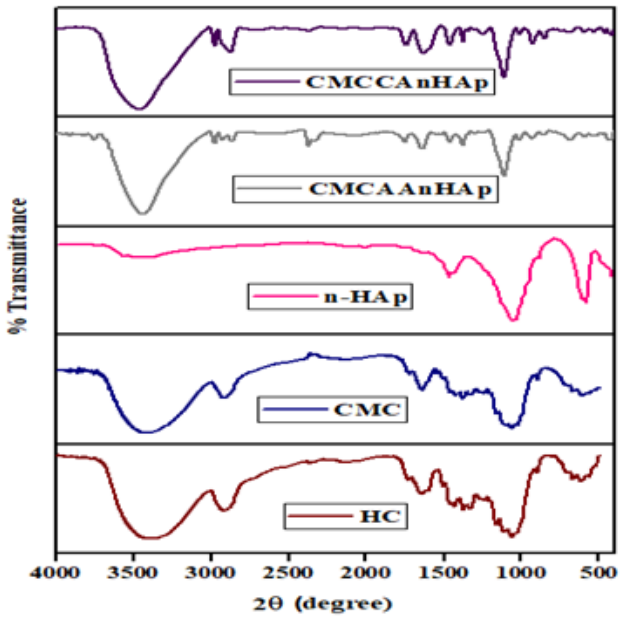

Fig 4. IR spectra for cellulose, CMC, n-HAp, CMC/AA/nHAp & CMC/CA/nHAp composites

4.2 XRD analysis

The X-Ray diffractogram for cellulose isolated from hemp, CMC, n-HAp and the composites CMC/AA/nHAp and CMC/CA/nHAp are shown in Figure 5. The average crystallite size of CMCs, n-HAp, CMC/AA/nHAp and CMC/CA/nHAp composite was calculated using scherrer's equation as 3.58nm, 19.9nm, 4.08nm, 25.85nm and 14.44nm respectively [17,21,29,47].

$$D = \frac{K\lambda}{\beta^{1/2}\cos\theta} \longrightarrow (1)$$

where λ is the wavelength ot x-rays, K is Scherrer's constant (0.94), $\beta^{1/2}$ is the peak's full width half maximum (FWHM), and θ is the Bragg's angle. The high vaule of percentage crystallinity of CMC showed the indication of effective hydrolysis which produces crystalline cellulose with removal of amorphous cellulose of chemically purified cellulose [18,37,44,59]. It could be observed that the crystallinity of the sample increases with the calcination temperature (500° C). The Ca/P stoichiometry of calcined HAp at 500° C temperature was analysed [23,36,45,49]. The typical peaks of AA and CA appeared in the diffraction patterns of the CMC/AA/nHAp and CMC/CA/nHAp composites after blending with CMC and HAp, showing that the crystal structure of the n-HAp in the composite did not change after blending. Crystallinity percentage of CMC/AA/nHAp and CMC/CA/nHAp composite were calculated and observed to increase because of CMCs strongly interacted with the hydroxyl groups of Agar-Agar and Carragenan [33,39,48,59]. The average crystallinity were found to be 47%, 58.3%, 55.3%, 52.2% and 40.25% for cellulose from hemp, CMC, nHAp, CMC/AA/nHAp and CMC/CA/nHAp composites respectively. The Crystallinity index of the cellulose, CMC, n-HAp, CMC/AA/nHAp, CMC/CA/nHAp were calculated by the following equation,

Crystallinity Index

$$(CI) = \frac{A_{crystalline}}{A_{amorphous} + A_{cryatalline}} \times 100 \quad (2)$$

where $A_{crystalline}$ is the area of crystalline curve, $A_{amorphous}$ is the area of amorphous curve.

TABLE 1 Average Crystallite Size, Crystallinity Index and 2θ values of Samples

S.No	Sources	Crystallinity Index (CI)	Average Crystallite Size (D)	2 θ Peaks
1	Cellulose from hemp	47%	3.58 nm	22.8°
2	CMC	49.3%	19.9 nm	36.9°
3	n-HAp	55.3%	4.08 nm	49.4°
4	CMC/AA/nHAp	46.2%	25.85 nm	45.67°
5	CMC/CA/nHAp	40.25%	14.44 nm	69.38°

The decrease in percentage crystallinity of composites shows their applications in medicinal field.

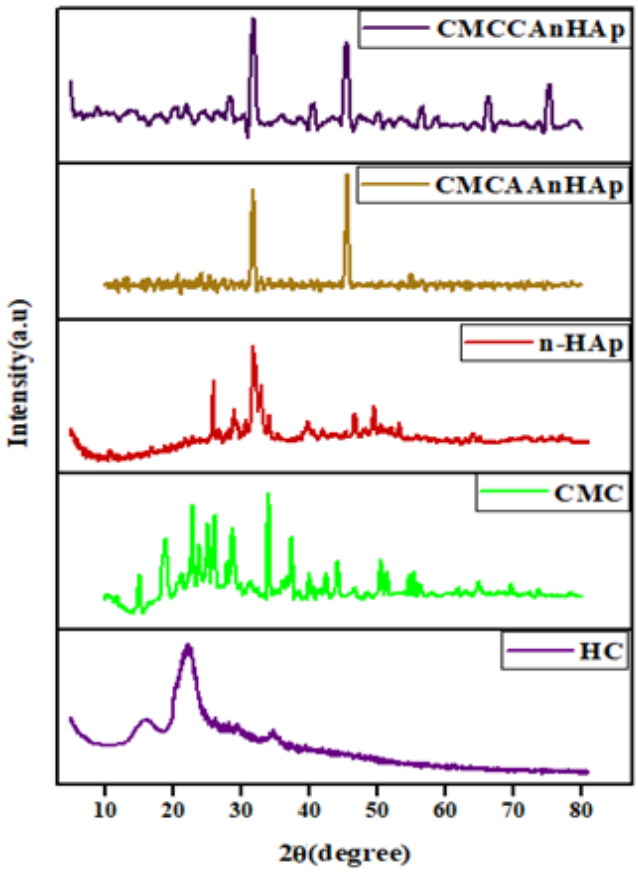

Fig 5. XRD patterns for prepared cellulose, CMC, n-HAp, CMC/AA/nHAp & CMC/ CA/nHAp composites

4.3 Morphology analysis

The study of Field Emission Scanning Electron Microscopy (FESEM) revealed more specific information about the shape and size features of the CMC, n-HAP particles contained in the film. For cellulose prepared from hemp, the fibres were stiff rod like structure and still intertwined with each other (Figure 6 a, b). The fibres were separated into smaller bundles and their size was in the micron range [12,15,19,33]. In CMC, at two different magnifications, the surface morphology in distinct locations shows a nearly smooth surface with layers of flakes as shown in fig 6 c,d. The outer surface was rough and twisted, which might be due to the alkaline and bleaching processes utilised in the cellulose extraction procedure [15,28,37,45]. The size of the CMC crystals ranges from 14nm to 20nm. The n-Hydroxyapatite powders looked to be in a smashed angular form, and a high magnification image revealed that each particle of nHAp is made up of nano-sized grains that appear as little brilliant spots and are pretty evenly spread over the image (Figure 6 e, f) [45,46,51,52]. The distribution of n-HAp particles in the composite film is seen in Figure 6 g, h, i, j. From the image it is very clear that the cubic shaped n-HAp particles are fairly well dispersed across the sample. There was no stacking found in the composite. The size of the n-HAp crystals ranges from 4nm to 10nm [15,24,33,46]. HAp particles can be homogeneously incorporated with Agar-agar/Carragenan and CMC matrix with good density, and the inorganic phase HAp bonding with organic phase in composite material with many small pores. The size of the CMC/AA/nHAp and CMC/CA/nHAP ranges from 21nm to 27nm and 12nm to 18nm respectively.

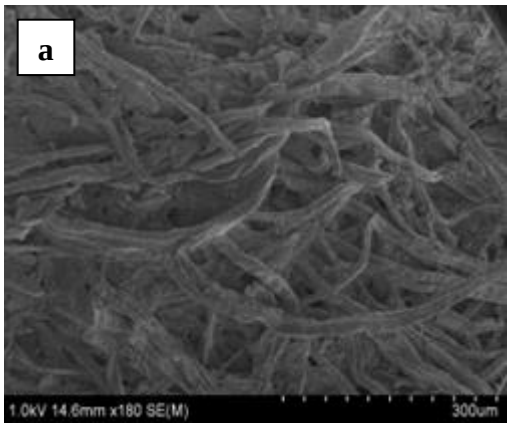

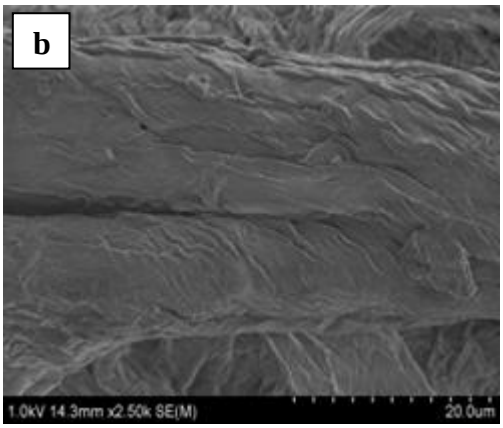

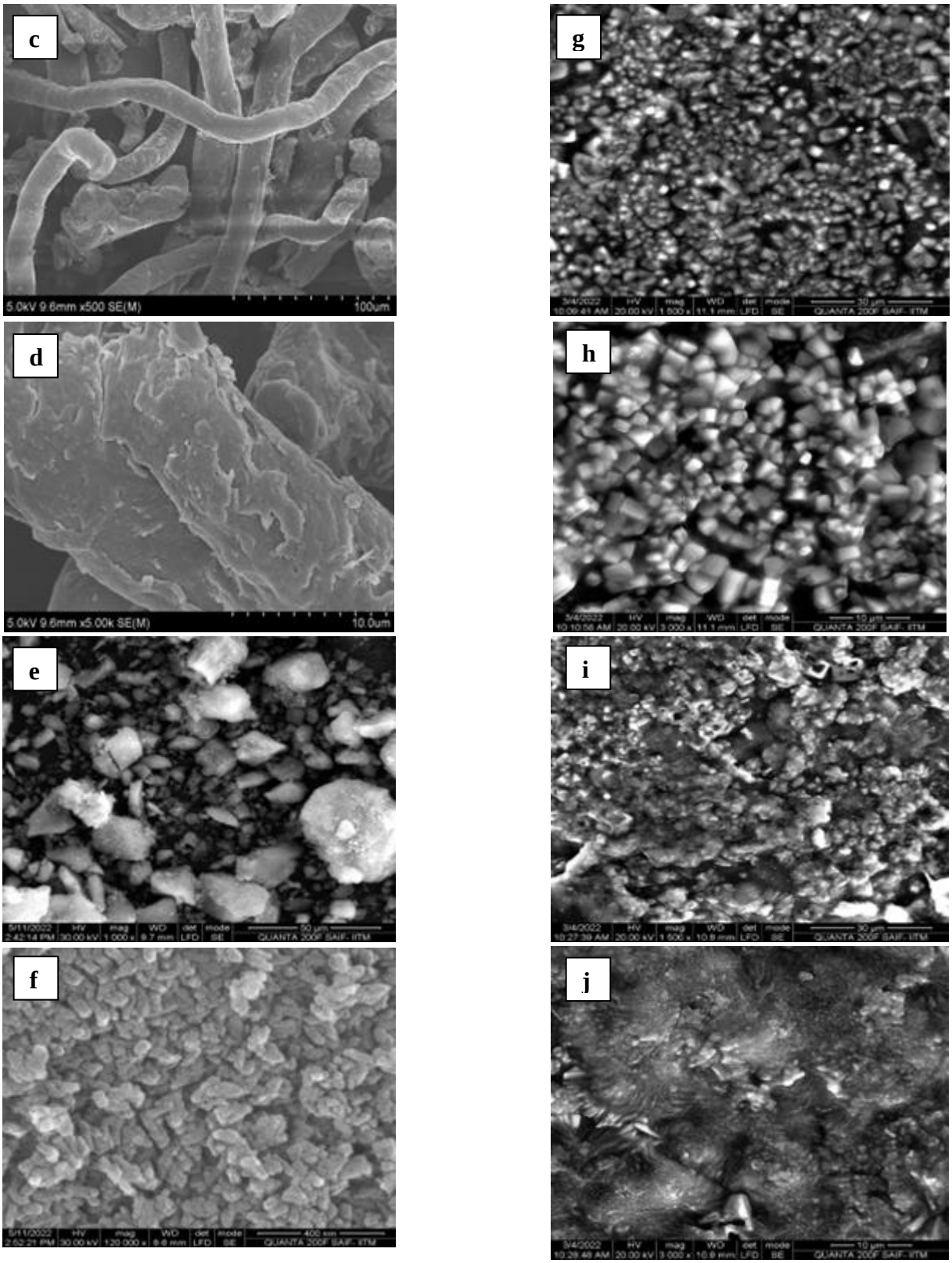

Fig 5. SEM images of (a,b) hemp (c,d) CMC (e,f) n-HAp (g,h) CMC/AA/nHAp (i,j) CMC/CA/nHAp

In comparison to CMC, composites shows morphological changes that confirms the interaction between the polymer and nano composites.

4.4 Energy Dispersive X-ray Spectroscopy

The EDS spectrum reveals the chemical composition of prepared CMC/AA/HAp and CMC/CA/HAp composites [18,22,25,28]. Figure shows the energy dispersive ray spectra of prepared composites, which confirms the elemental composition of composite films. The EDS analysis confirms the presence of C, N, O, Na, P, Cl, Ca.

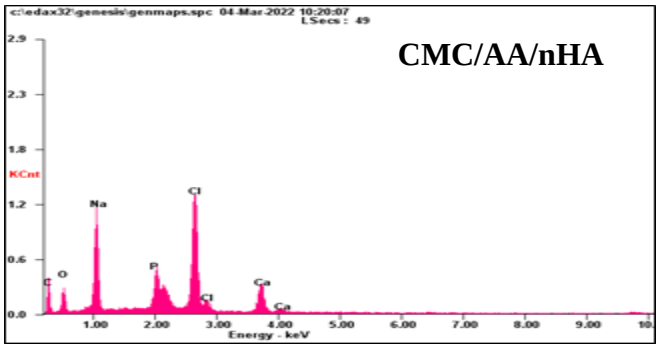

Sample	Element	Weight %	Atomic %
CMC/AA/ nHAp	C	42.83	60.61
	O	13.67	14.53
	Na	15.11	11.17
	Mg	00.25	00.17
	P	05.05	02.77
	Ca	05.93	02.52

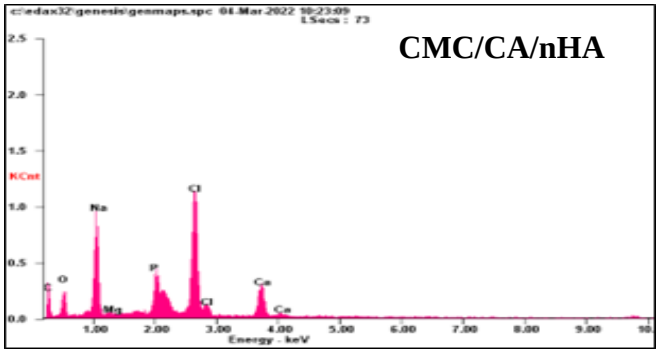

Sample	Element	Weight %	Atomic %
CMC/CA/ nHAp	C	26.51	41.49
	O	28.03	32.93
	Na	05.57	04.55
	P	12.00	07.28
	Cl	10.18	05.40
	K	02.66	01.28

Fig 7. EDS Spectrum and Elemental percentage composition of CMC/AA/nHAp & CMC/CA/nHAp composites

4.5 Thermal analysis

Thermogravimetric (TG) and Derivative Thermogravimetric (DTG) analysis were carried out in the range of 5°C to 600°C to evaluate the thermal stability and understand the phase changes of the prepared samples. The TGA and DTA thermograms recorded for the samples are shown in Figure 8. The moisture in the sample shown by the initial weight loss, occurred at 96°C [9,13,23,44]. The second weight loss occurred between 185°C and 390°C, indicating that cellulose is thermally stable. The evaporation of water molecule shows an endothermic peak at 109°C. A significant peak at 371.7°C for degradation, confirms the existence of cellulose isolated from hemp. The major decomposition of cellulose begins around 270°C, with a weight loss of 20% attributed to the inorganic moiety and a minimum weight loss of 10.40% beginning at 154°C [11,26,33,57]. The dehydration of the precipitating complex and the loss of physically adsorbed water molecules of the hydroxyapatite powder correlate to the first endothermic peak, which ranges from 90 to 295°C [35,45,51] with a peak at around 250°C [33,47,49]. This area has lost 16 percent of its weight. There was no peak with rising temperature from 295°C, except for a weight loss at the TGA curve in the temperature range, which is thought to be due to progressive dehydroxyllin in hydroxyapatite powder. For the composite CMCAAHAp, the first weight loss occurs at 150°C, was for the surface

adsorbed water molecules. The second weight loss occurs at 400°C confirms the degradation of Biopolymer [31,36,55]. The third inflexion point occurs at 800°C shows the degradation of n-HAp. The first weight loss occurs at 120°C, was for the surface adsorbed water molecules. The second weight loss occurs at 400°C to 450°C confirms the degradation of Biopolymer. The third weight loss starts at 600°C shows the degradation of n-HAp.

Table 2 Glass transition temperature (T_g), Melting temperature (T_m) and decomposition temperature (T_d) for cellulose, CMC, n-HAp, CMC/AA/nHAp and CMC/CA/nHAp composites

S.No	Sample	T_g (°C)	T_m (°C)	T_d (°C)
1	Cellulose from Hemp	75°C	383°C	391°C
2	CMC	78°C	275°C	380°C
3	n-HAp	-	238°C	290°C
4	CMC/AA/nHAp	45°C	220°C	260°C
5	CMC/CA/nHAp	40°C	189°C	225°C

The thermal parameters such as glass transition temperature (T_g), melting temperature (T_m) and decomposition temperature (T_d) are presented in table 2.

The glass transition temperature (T_g) values of the composites are lower than the CMC and n-HAp. This shows that these composites are more flexible which is one of the major criteria for designing thin films. Also the melting temperature (T_m) and decomposition temperature (T_d) are comparatively high which shows that the prepared composites are thermally stable.

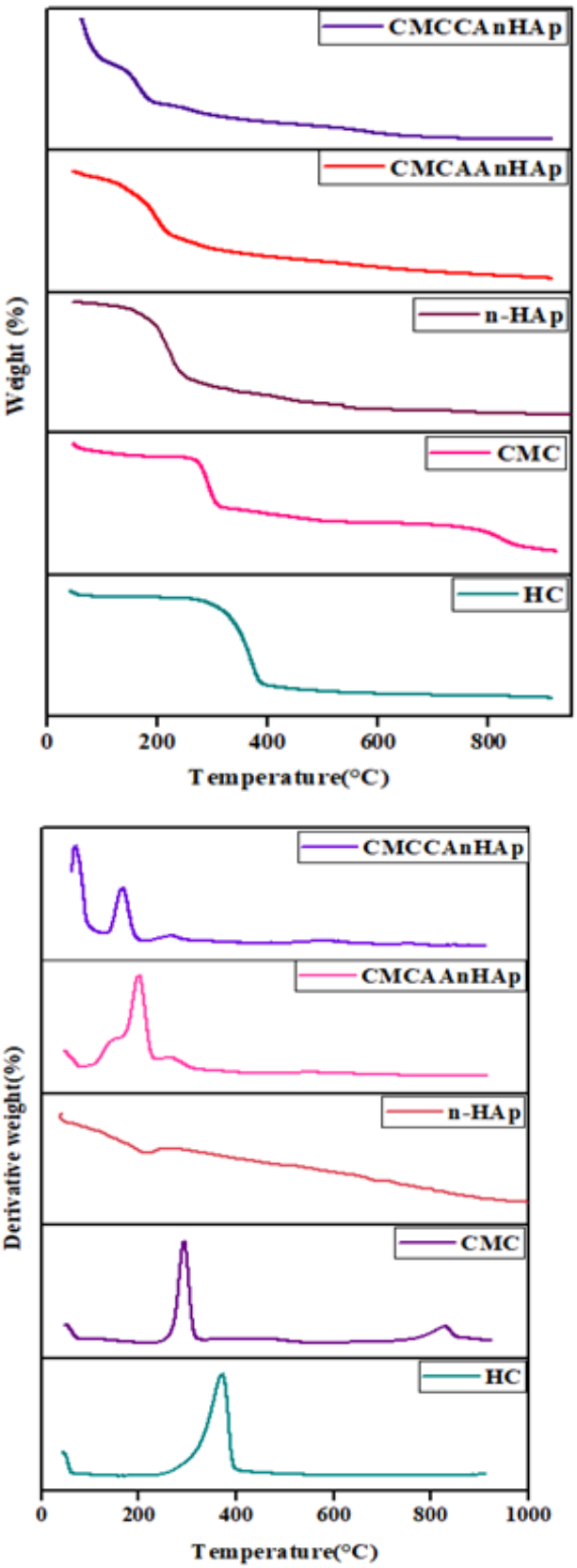

Fig 8. TGA & DTA thermograms for cellulose, CMC, n-HAp, CMC/AA/nHAp & CMC/CA/nHAp composites

4.6 Biomedical Applications

4.6.1 Antibacterial Activity

Antibacterial activity of the samples was determined by disc diffusion method on Muller Hinton agar (MHA) medium for CMC/AA/nHAp and CMC/CA/nHAp composite films. Muller Hinton Agar (MHA) medium is poured in to the petri plate [40,44,52]. After the medium was solidified, the inoculums were spread on the solid plates with sterile swab moistened with the bacterial suspension. The discs were placed in MHA plates and add 20 µl of sample Concentration: 1000µg, 750µg and 500 µg were placed in the disc (Figure 9). The plates were incubated at 37ºC for 24 hrs [42,55,59]. Then the antimicrobial activity was determined by measuring the diameter of zone of inhibition.

Table 2 Zone of Inhibition of bacteria in 1000, 750, 500 µg/ml for CMC/AA/nHAp composite Film

Organisms	Zone of Inhibition(mm) Sample (µg/ml)			Antibiotic (1mg/ml)
	1000	750	500	
Staphylococcus aureus	-	-	-	26
Pseudomonas aeruginosa	14	11	7	39
Enterococcus faecalis	22	18	10	47
Bacillus subtilis	7	-	-	33
Escherichia coli	-	-	-	7

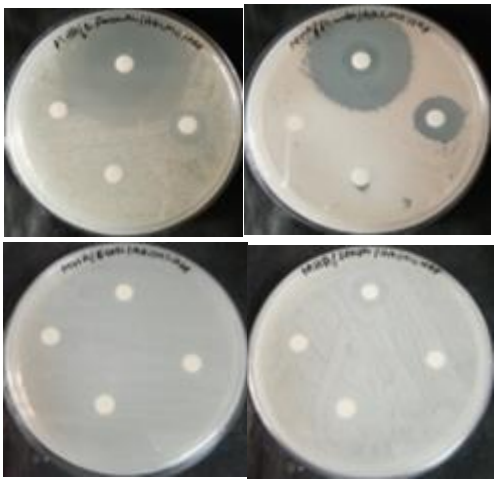

Fig 9. Images of Zone of Inhibition of *Enterococcus faecalis, Pseudomonas aeruginosa, Escherichia coli, Staphylococcus aureus, Bacillus subtilis* in 1000, 750, 500 µg/ml

The result showed that *Enterococcus faecalis* has better antibacterial activity in 1000, 750, 500 µg/ml in CMC/AA/nHAp composite film.

Table 3 Zone of Inhibition of bacteria in 1000, 750, 500 µg/ml for CMC/CA/nHAp composite Film

Organisms	Zone of Inhibition(mm) Sample (µg/ml)			Antibiotic (1mg/ml)
	1000	750	500	
Staphylococcus aureus	-	-	-	14
Pseudomonas aeruginosa	17	8	7	36
Enterococcus faecalis	12	9	8	46
Bacillus subtilis	-	-	-	32
Escherichia.coli	-	-	-	7

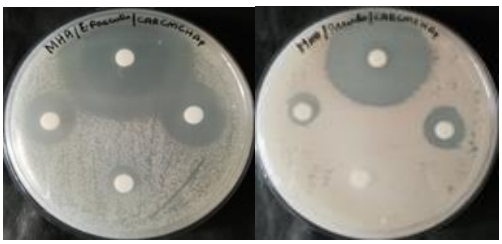

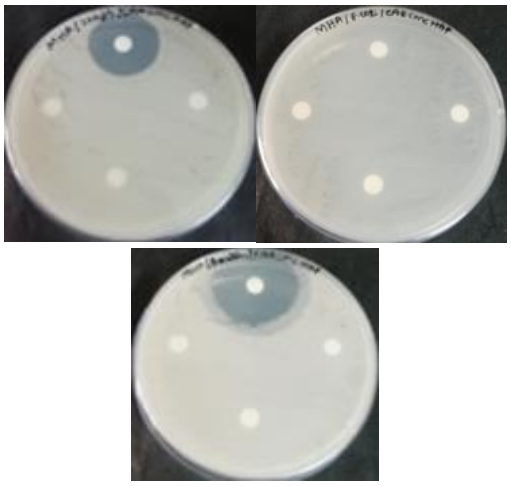

Fig 10. Images of Zone of Inhibition of *Enterococcus faecalis, Pseudomonas aeruginosa, Staphylococcus aureus, Escherichia coli, Bacillus subtilis* in 1000, 750, 500 µg/ml

The result showed that *Enterococcus faecalis* has better antibacterial activity in 1000, 750, 500 µg/ml in CMC/CA/nHAp composite film.

4.6.2 Antifungal Activity

Agar disc diffusion method

Antifungal activity of the Sample was determined by disc diffusion method on Sabouraud Dextrose agar (SDA) medium for CMC/AA/nHAp and CMC/CA/nHAp composites. Sabouraud Dextrose agar (SDA) medium is poured in to the petriplate [31,38,43]. After the medium was solidified, the inoculums were spread on the solid plates with sterile swab moistened with the fungal suspension. Amphotericin-B is taken as positive control. Samples and positive control of 20 µl each were added in sterile discs and placed in SDA plates [38,40,42]. The plates were incubated at 28ºC for 24 hrs (Figure 11). Then antifungal activity was determined by measuring the diameter of zone of inhibition.

Table 4 Zone of Inhibition of fungi in 1000, 750, 500 µg/ml for CMC/AA/nHAp composite Films

Organisms	Zone of Inhibition(mm)			Antibiotic (1mg/ml)
	Sample (µg/ml)			
	1000	750	500	
Trichoderma viride	8	7	7	8
Rhizopus stolonifer	-	7	-	7
Candida albicans	8	7	-	10

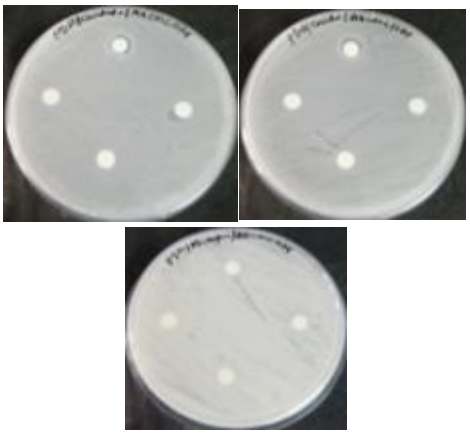

Fig 11. Images of Zone of Inhibition of *Trichoderma viride, Candida albicans, Rhizopus stolonifer* in 1000, 750, 500 µg/ml

The result showed that *Candida albicans* has better activity in 1000, 750, 500 µg/ml in CMC/AA/nHAp composite films.

Table 5 Zone of Inhibition of fungi in 1000, 750, 500 µg/ml for CMC/CA/nHAp composite Films

Organisms	Zone of Inhibition(mm)			Antibiotic (1mg/ml)
	Sample (µg/ml)			
	1000	750	500	
Trichoderma viride	8	7	7	8

S.No	Sample	Measurement (%)
1	CMC/CA/nHAp	**0.66**
2	CMC/AA/nHAp	**0.50**
3	Control	**0.72**

Rhizopus stolonifer	8	-	-	8
Candida albicans	8	7	-	10

Fig 12. Images of Zone of Inhibition of *Trichoderma viride, Candida albicans, Rhizopus stolonifer* in 1000, 750, 500 µg/ml

The result showed that *Candida albicans* has better activity in 1000, 750, 500 µg/ml in CMC/CA/nHAp composite films.

4.6.3 Wound Healing Activity

The VERO cell line was used to check the Wound healing activity for CMC/AA/nHAp and CMC/CA/nHAp composites [11,40,42,]. The cells were seeded into the 6-well plate and incubated for 24 hrs. After incubation, the cells were observed for growth and assay was preceded. The medium was discarded and the plate was kept under microscope. A sterile tip was used and wound was created and wells were washed with sterile PBS in order to wash the detached cells. 1 ml of the sample was added to the well and incubated. Control well (without the sample) was also maintained [30-32,52]. After 24 hrs of incubation, the plate was observed for the growth of cells (Figure 13). The wound created time is considered as the measurement at the 0th hour. The wound closure percentage of the cells are calculated using the formulae,

$$\text{Wound Closure \%} = \frac{\text{Measurement at } 0^{th} \text{ hour} - \text{Measurement at } 24^{th} \text{ hour}}{\text{Measurement at } 0^{th} \text{ hour}} \times 100 \longrightarrow (3)$$

Table 6 Wound closure measurement for CMC/AA/nHAp & CMC/CA/nHAp composite

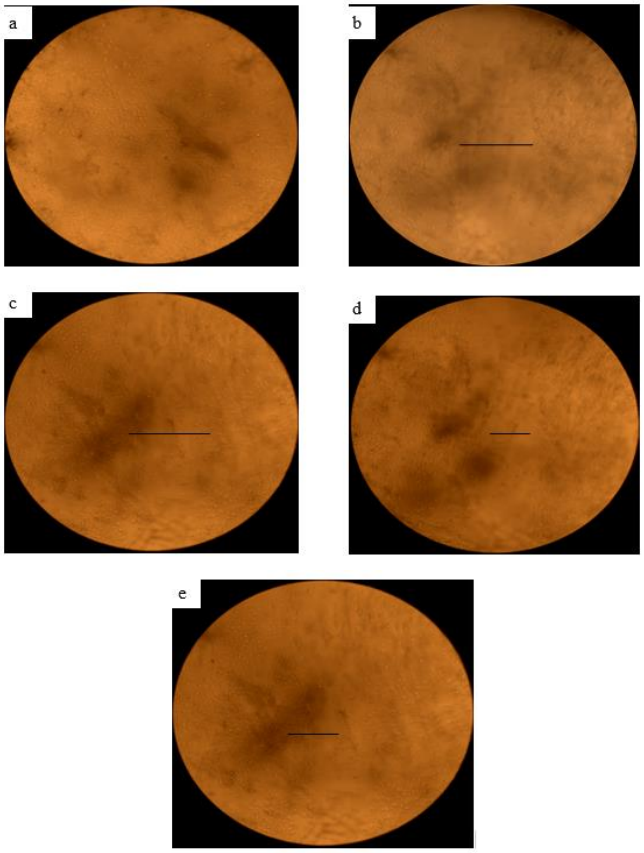

Fig 13. Images of wound healing activity of a. Normal cell line b. Wound created c. Control cell line d. CMC/AA/nHAp e. CMC/CA/nHAp

4.6.4 Anticancer Activity

Cells (1×10^5/well) were plated in 24-well plates and incubated in 37^0C with 5% CO_2 condition. After the cell reaches the confluence, the various concentrations of the samples were added and incubated for 24hrs [46,50,55]. After incubation, the sample was removed from the well and washed with phosphate-buffered saline (pH 7.4). 100µl/well (5mg/ml) of 0.5% 3-(4,5-dimethyl-2-thiazolyl)-2,5-diphenyl--tetrazolium bromide (MTT) was added and incubated for 4 hours [23,27,33,40]. After incubation, 1ml of DMSO was added in all the wells .The absorbance at 570nm was measured with UV- Spectrophotometer using DMSO as the blank. Measurements were performed and the concentration required for a 50% inhibition (IC50) was

determined graphically. The % cell viability was calculated using the following formula:

% Cell viability = A570 of treated cells / A570 of control cells × 100 **(4)**

Graphs are plotted using the % of Cell Viability at Y-axis and concentration of the sample in X-axis [42,43]. Cell control and sample control is included in each assay to compare the full cell viability assessments.

Table 7 Anticancer effect of CMC/AA/nHAp *on MCF 7* cell line

S.No	Concentration (µg/ml)	Dilutions	Absorbance (O.D)	Cell Viability (%)
1	1000	Neat	0.207	50.61
2	500	1:1	0.241	58.92
3	250	1:2	0.274	66.99
4	125	1:4	0.308	75.30
5	62.5	1:8	0.341	83.37
6	31.2	1:16	0.376	89.93
7	15.6	1:32	0.412	93.73
8	7.8	1:64	0.445	98.80
9	Cell control	-	0.409	100

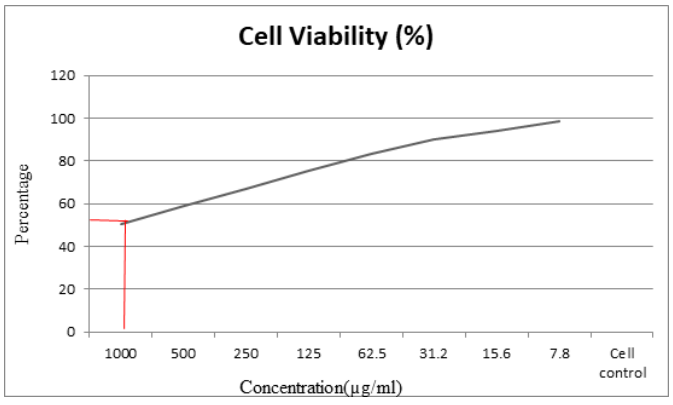

Fig 14. Percentage Cell viability for CMC/AA/nHAp composite

Table 8 Anticancer effect of CMC/CA/nHAp *on MCF 7* cell line

S.No	Concentration (µg/ml)	Dilutions	Absorbance (O.D)	Cell Viability (%)
1	1000	Neat	0.164	30.20
2	500	1:1	0.275	50.64
3	250	1:2	0.323	59.48
4	125	1:4	0.371	68.32
5	62.5	1:8	0.418	76.97
6	31.2	1:16	0.465	85.63
7	15.6	1:32	0.512	91.29
8	7.8	1:64	0.560	98.6
9	Cell control	-	0.453	100

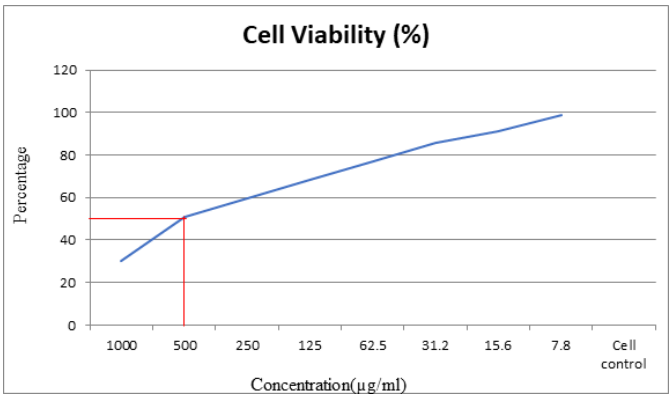

Fig 14. Percentage Cell viability for CMC/CA/nHAp composite

V. CONCLUSION

In this investigation, we reported the preparation, characterisation and antimicrobial studies of n-hydroxyapatite (n-HAp) incorporated carboxymethyl cellulose and Agar-Agar/I-Carragenan composites. The prepared composites were structurally analysed using FT-IR, XRD and TGA/DTA techniques as well as morphology using HR-SEM analysis. The addition of nano hydroxyapatite particles in the polymer matrix altered the morphology. The antimicrobial studies such as antibacterial, antifungal, wound healing and anticancer activities were evaluated with the prepared

composite materials. The results showed that the composite materials posses inhibition against pathogens. This research demonstrates that the CMC/Agar-Agar/nHAp and CMC/I-Carragenan/nHAp nanocomposites are potential biomaterials for appropriate biomedical applications.

Acknowledgement

We are acknowledging Dr. Amirthavalli Raghupathy Memorial Fund for providing support (Muffle Furnace Instrument) for our research laboratory. Also, authors would like to acknowledge Department of chemistry, IIT Madras, for providing characterisation facility.

Conflict of interest

The authors declare that they have no conflict of interest.

VI. REFERENCES

[1]. Karthika Ammini Sindhu, Raghavan Prasanth, Vijay Kumar Thakur, Medical Applications of Cellulose and Its Derivatives: Present and Future Nanocellulose Polymer Nanocomposites, 2015, 437-478.

[2]. Hadi Seddiqi, Erfan Oliaei, Hengameh Honarkar, Jianfeng Jin, Lester C. Geonzon, Rommel G. Bacabac , Jenneke Klein-Nulend, Cellulose and its derivatives: towards biomedical applications Cellulose, 28, 2021, 1893–1931.

[3]. Ahmed Salama, Cellulose/calcium phosphate hybrids: New materials for biomedical and environmental applications, International Journal of Biological Macromolecules, 127, 2017, 606 – 617.

[4]. A. Shalini, P. Paulraj, K. Pandian, G. Anbalagan, V. Jaisankar, Single pot synthesis, characterization of PPy@C composites modified electrode for the electrocatalytic determination of ascorbic acid in commercial fruit samples, Surfaces and interfaces, 17, 2019, 100386.

[5]. Nadezda Stevulova, Julia Cigasova, Adriana Estokova, Eva Terpakova, Anton Geffert, Frantisek Kacik, Eva Singovszka and Marian Holub, Properties Characterization of Chemically Modified Hemp Hurds, Materials, 7, 2014, 8131-8150.

[6]. Silvana Mueler, Christoph Weder, E. Johan Foster, Isolation of Cellulose Nanocrystals from Pseudostems of banana plants, RSC Advances, 4, 2014, 907-915.

[7]. Lakshmipriya Ravindran, Sreekala M.S., Sabu Thomas, Novel processing parameters for the extraction of cellulose nanofibres (CNF) from environmentally benign pineapple leaf fibres (PALF): Structure-property relationships, International Journal of Biological Macromolecules, 131, 2019, 858–870.

[8]. M. Sasikala, M. J. Umapathy, Preparation and characterization of pineapple leaf cellulose nanocrystal reinforced gelatin bio-nanocomposite with antibacterial banana leaf extract for application in food packaging, New J. Chem, 42, 2018, 19979-19986.

[9]. Kumar, Anuj, Y. S. Negi, N. K. Bhardwaj, and V. Choudhary, Synthesis and Characterization of Cellulose Nanocrystals/PVA Based Bionanocomposite, Advanced Materials Letters, 4.8, 2013, 626–31.

[10]. Sasikala, M., and M. J. Umapathy, Preparation and Characterization of Pineapple Leaf Cellulose Nanocrystal Reinforced Gelatin Bio-Nanocomposite with Antibacterial Banana Leaf Extract for Application in Food Packaging, New Journal of Chemistry, 42.24, 2018, 19979–86.

[11]. Nomura, Kazumasa, Paul Terwilliger, and A A We, Self-Dual Leonard Pairs Modifications of Microcrystalline Cellulose Cellulose (NFC) and Cellulose (NCC) for Antimicrobial and Wound Healing Applications A, 2019.

[12]. Ragu, A, K Senthilarasan, and P Sakthivel, Synthesis and Characterization of Nano Hydroxyapatite with Polyurethane Nano Composite, Joural of Scientific and Research Publications, 4.2, 2014, 2–4.

[13]. Santos, Roni Marcos dos, Wilson Pires Flauzino Neto, Hudson Alves Silvério, Douglas Ferreira

Martins, Noélio Oliveira Dantas, and Daniel Pasquini, Cellulose Nanocrystals from Pineapple Leaf, a New Approach for the Reuse of This Agro-Waste, Industrial Crops and Products, 50, 2013, 707–14.

[14]. Ioelovich, Michael, Cellulose: Nanostructured Natural Polymer Michael Ioelovich, 2014.

[15]. Li, Meng, Yan Ling Cheng, Nan Fu, Dong Li, Benu Adhikari, and Xiao Dong Chen, Isolation and Characterization of Corncob Cellulose Fibers Using Microwave-Assisted Chemical Treatments, International Journal of Food Engineering, 10.3, 2014, 427–36.

[16]. Jonoobi, Mehdi, Reza Oladi, Yalda Davoudpour, Kristiina Oksman, Alain Dufresne, Yahya Hamzeh, and others, Different Preparation Methods and Properties of Nanostructured Cellulose from Various Natural Resources and Residues: A Review, Cellulose, 22.2, 2015, 935–69

[17]. Cherian, Bibin Mathew, Alcides Lopes Leão, Sivoney Ferreira de Souza, Sabu Thomas, Laly A. Pothan, and M. Kottaisamy, Isolation of Nanocellulose from Pineapple Leaf Fibres by Steam Explosion, Carbohydrate Polymers, 81.3, 2010, 720–25

[18]. Sai Prasanna, N., and Jayeeta Mitra, Isolation and Characterization of Cellulose Nanocrystals from Cucumis Sativus Peels, Carbohydrate Polymers, 247, 2020, 116706.

[19]. Abral, H., Putra, G. J., Asrofi, M., Park, J.-W., & Kim, H.-J., Effect of vibration duration of high ultrasound applied to bio-composite while gelatinized on its properties, Ultrasonics Sonochemistry, 40, 2018, 697–702.

[20]. Asrofi, M., Abral, H., Kasim, A., Pratoto, A., & Mahardika, M. Isolation of nanocellulose from water hyacinth fiber (WHF) produced via digester-sonication and its characterization, Fibers and Polymers, 19, 2018, 1618–1625.

[21]. Julie Chandra, C. S., George, N., & Narayanankutty, S. K. Isolation and characterization of cellulose nanofibrils from arecanut husk fibre. Carbohydrate Polymers, 142, 2016, 158–166.

[22]. Cheng, Q., Wang, S., & Han, Q., Novel process for isolating fibrils from cellulose fibers by high-intensity ultrasonication. II. fibril characterization. Journal of Applied Polymer Science, 115, 2010, 2756–2762.

[23]. Farahbakhsh, N., Venditti, R. A., and Jur, J. S. Mechanical and thermal investigation of thermoplastic nanocomposite films fabricated using micro- and nano-sized fillers from recycled cotton T-shirts. Cellulose, 21, 2014, 2743–2755.

[24]. Johar, N., Ahmad, I., & Dufresne, A. Extraction, preparation and characterization of cellulose fibres and nanocrystals from rice husk. Industrial Crops and Products, 37(1), 2012, 93–99.

[25]. Mahardika, M., Abral, H., Kasim, A., Arief, S., & Asrofi, M. Production of nanocellulose from pineapple leaf fibers via high-shear homogenization and ultrasonication. Fibers, 6(2), 2018, 28.

[26]. Ng, H. M., Sin, L. T., Tee, T. T., Bee, S. T., Hui, D., Low, C. Y., Extraction of cellulose nanocrystals from plant sources for application as reinforcing agent in polymers. Composites Part B: Engineering, 75, 2015, 176–200.

[27]. Rafi, M., Lim, L. W., Takeuchi, T., & Darusman, L. K. Simultaneous determination of gingerols and shogaol using capillary liquid chromatography and its application in discrimination of three ginger varieties from Indonesia. Talanta, 103, 2013, 28–32.

[28]. Song, J., Chen, C., Zhu, S., Zhu, M., Dai, J., Ray, U. Hu, L. Processing bulk natural wood into a high-performance structural material. Nature, 554, 2018, 224–228.

[29]. Wei, Wenbang, Wei Song, and Shuangbao Zhang, Preparation and Characterization of Hydroxyapatite-Poly(Vinyl Alcohol) Composites Reinforced with Cellulose Nanocrystals, BioResources, 9.4, 2014, 6087–99.

[30]. Jacob, Joby, Gregary Peter, Sabu Thomas, Józef T. Haponiuk, and Sreeraj Gopi, Chitosan and Polyvinyl Alcohol Nanocomposites with Cellulose Nanofibers from Ginger Rhizomes and Its

Antimicrobial Activities, International Journal of Biological Macromolecules, 129, 2019, 370–76.

[31]. Luo, X., Li, J., Lin, X. Effect of gelatinization and additives on morphology and thermal behavior of corn starch/PVA blend films. Carbohydr. Polym. 2012, 90, 1595–1600.

[32]. Yuan, P., Tan, D., Annabi-Bergaya, F. Properties and applications of halloysite nanotubes: Recent research advances and future prospects. Appl. Clay Sci. 2015, 112–113, 75–93.

[33]. Jang, J.,Lee, D.K. Plasticizer effect on the melting and crystallization behavior of polyvinyl alcohol. Polymer 2003, 44, 8139–8146

[34]. Negim, E.S.M., Rakhmetullayeva, R.K., Yeligbayeva, G.Zh., Urkimbaeva, P.I., Primzharova, S.T., Kaldybekov, D.B., Khatib, J.M., Mun, G.A., Craig, W. Improving biodegradability of polyvinyl alcohol/starch blend films for packaging applications. Int. J. Basic Appl. Sci. 2014, 3, 263–273.

[35]. Roohani, M., Habibi, Y., Belgacem, N.M., Ebrahim, G., Karimi, A.N., Dufresne, A. Cellulose whiskers reinforced polyvinyl alcohol copolymers nanocomposites. Eur. Polym. J. 2008, 44, 2489–2498.

[36]. Yao , Q. , Yang , Y. , Pu , X. , Yang , L. , Hou , Z. , Dong , Y. , Zhang , Q. Preparation, characterization and osteoblastic activity of chitosan/polycaprolactone/in situ hydroxyapatite scaffolds . J. Biomater. Sci. Polym. Ed. 2012, 23, 1755 – 1770.

[37]. Deng , C. , Wang , B. , Dongqin , X. , Zhou , S. , Duan , K. , Weng , J. Preparation and shape memory property of hydroxyapatite/poly (vinyl alcohol) composite . Polym.-Plast. Technol. Eng. 2012, 51 , 1315 – 1318

[38]. Collins, C.H. , Lyne , P.M. Microbiological Methods, , 5th Ed. , Butterworth and Co. Ltd. : London and Toronto , 1985, pp. 167 – 181.

[39]. Youssef , A.M. , Abdel-Aziz , M.S. Preparation of polystyrene nanocomposites based on silver nanoparticles using marine bacterium for packaging . Polym.-Plast. Technol. Eng. 2013, 52, 607 – 613.

[40]. He , S. Guo , Z. , Zhang , Y. , Zhang , S. , Gu , J.W. Biosynthesis of gold nanoparticles using the bacteria Rhodopseudomonas capsulata . Mater. Lett. 2007, 61, 3984 – 3987.

[41]. Ahmad , A. , Mukherjee , P. , Senapati , S. , Mandal , D. , Khan , M.I. , Kumar , R. , Sastry , M. Extracellular biosynthesis of silver nanoparticles using the fungus Fusarium oxysporum . Coll. Surf. B-Biointerf. 2003, 28, 313 – 318.

[42]. Senapati , S. , Ahmad , A. , Khan , M.I. , Sastry , M. , Kumar , R. Extracellular biosynthesis of bimetallic Au-Ag alloy nanoparticles . Small 2005, 1, 517 – 520.

[43]. Mulvaney, P. Surface plasmon spectroscopy of nanosized metal particles . Langmuir 1996, 12, 788 – 800.

[44]. Balagurunathan, R. , Radhakrishnan, M. , Rajendran, R.B. , Velmurugan, D. Biosynthesis of gold nanoparticles by actinomycete Streptomyces viridogens strain HM10 . Ind. J. Biochem. Biophys. 2011, 48, 331 – 335.

[45]. Anee , T.K. , Ashok , M. , Palanichamy , M. , Kalkura , S.N. A novel technique to synthesize hydroxyapatite at low temperature . Mater. Chem. Phys. 2003, 80, 725 – 730.

[46]. Liu , Y. , Hou , D. , Wang , G. A simple wet chemical synthesis and characterization of hydroxyapatite nanorods . Mater. Chem. Phys. 2004, 86, 69 – 73.

[47]. Katti , S.K. Static and dynamic mechanical behavior of hydroxyapatite-polyacrylic acid composites under simulated body fluid . J. Amer. Bioch. Biotech. 2006, 2, 73 – 79.

[48]. Musterman, Max, and Paul Placeholder, About of The Preparation and Antibacterial Activity Cellulose / ZnO Composite : A Review What Is So Different About Was Ist so Anders Am Neuroenhancement, Open Chemistry, 12.2, 2018, 9–20.

[49]. Wang, Dong, W. Cheng, Qingxiang Wang, Junjiao Zang, Yan Zhang, and Guangping Han, Preparation of Electrospun Chitosan/Poly(Ethylene Oxide) Composite Nanofibers Reinforced with Cellulose

Nanocrystals: Structure, Morphology, and Mechanical Behavior, Composites Science and Technology, 182, 2019, 107774.

[50]. Rahman, Mohammed Mizanur, Sanjida Afrin, and Papia Haque, Characterization of Crystalline Cellulose of Jute Reinforced Poly (Vinyl Alcohol) (PVA) Biocomposite Film for Potential Biomedical Applications, Progress in Biomaterials, 3.1, 2014.

[51]. Wei, Wenbang, Wei Song, and Shuangbao Zhang, Preparation and Characterization of Hydroxyapatite-Poly(Vinyl Alcohol) Composites Reinforced with Cellulose Nanocrystals, BioResources, 9.4, 2014, 6087–99.

[52]. Sivasankari, Selvam, Rajappan Kalaivizhi, Natesan Gowriboy, Munuswamy Ramanujam Ganesh, and Musthafa Shazia Anjum, Hydroxyapatite Integrated with Cellulose Acetate/Polyetherimide Composite Membrane for Biomedical Applications, Polymer Composites, 42.10, 2021, 5512–26.

[53]. Noronha, Victor T., Camilla H.M. Camargos, Jennifer C. Jackson, Antonio G. Souza Filho, Amauri J. Paula, Camila A. Rezende, and others, Physical Membrane-Stress-Mediated Antimicrobial Properties of Cellulose Nanocrystals, ACS Sustainable Chemistry and Engineering, 9.8, 2021, 3203–12.

[54]. Millon, L. E., and W. K. Wan, The Polyvinyl Alcohol-Bacterial Cellulose System as a New Nanocomposite for Biomedical Applications, Journal of Biomedical Materials Research - Part B Applied Biomaterials, 79.2, 2006, 245–53.

[55]. Kamoun, Elbadawy A., El Refaie S. Kenawy, and Xin Chen, A Review on Polymeric Hydrogel Membranes for Wound Dressing Applications: PVA-Based Hydrogel Dressings, Journal of Advanced Research, 8.3, 2017, 217–33.

[56]. Gan, Ivy, and W. S. Chow, Antimicrobial Poly(Lactic Acid)/Cellulose Bionanocomposite for Food Packaging Application: A Review, Food Packaging and Shelf Life, 2018, 150–61.

[57]. Farooq, Amjad, Mohammed Kayes Patoary, Meiling Zhang, Hassan Mussana, Mengmeng Li, Muhammad Awais Naeem, and others, Cellulose from Sources to Nanocellulose and an Overview of Synthesis and Properties of Nanocellulose/Zinc Oxide Nanocomposite Materials, International Journal of Biological Macromolecules, 154, 2020, 1050–73.

[58]. Edikresnha, Dhewa, Tri Suciati, Muhammad Miftahul Munir, and Khairurrijal Khairurrijal, Polyvinylpyrrolidone/Cellulose Acetate Electrospun Composite Nanofibres Loaded by Glycerine and Garlic Extract with: In Vitro Antibacterial Activity and Release Behaviour Test, RSC Advances, 9.45, 2019, 26351–63.

[59]. Abral, Hairul, Jeri Ariksa, M. Mahardika, Dian Handayani, Ibtisamatul Aminah, Neny Sandrawati, and others, Transparent and Antimicrobial Cellulose Film from Ginger Nanofiber, Food Hydrocolloids, 98, 2020, 105266.

Cite this Article

Kiruthika T. S, Aravind Viswanath J, Jaishankar V, "Hydroxyapatite integrated with Carboxymethyl cellulose and Agar-Agar/I-Carragenan biopolymer composites for antimicrobial investigations", International Journal of Scientific Research in Science, Engineering and Technology (IJSRSET), Online ISSN : 2394-4099, Print ISSN : 2395-1990, Volume 9 Issue 4, pp. 86-103, July-August 2022. Available at doi : https://doi.org/10.32628/IJSRSET229410
Journal URL : https://ijsrset.com/IJSRSET229410